Marine Structures 84 (2022) 103189

Contents lists available at ScienceDirect

Marine Structures

journal homepage: www.elsevier.com/locate/marstruc

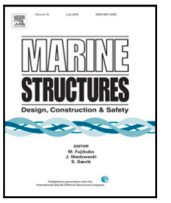

Mooring system stiffness: A six-degree-of-freedom closed-form analytical formulation

Giovanni A. Amaral *, Celso P. Pesce, Guilherme R. Franzini

LMO – Offshore Mechanics Laboratory, Escola Politécnica, University of São Paulo, Av. Prof. Lúcio Martins Rodrigues, Tv. 4, 434, São Paulo 05508-020, Brazil

ARTICLE INFO

Keywords:
Mooring system
Stiffness matrix
Analytical formulation
Natural periods
Coupling effects

ABSTRACT

A mooring system project is an iterative process, involving design and analysis with numerous parameters. In this context, analytical tools can help to reduce the use of expensive and time consuming full nonlinear numerical simulations based on high-order hierarchical models such as Finite Element models, mainly during early stages of the design. By employing Analytical Mechanics approaches, the present article brings an analytical and closed-mathematical-form formulation to determine the six-degree-of-freedom (DOF) mooring system stiffness matrix at any generic position of the floating body, provided mooring line forces are modeled as conservative ones. In order to demonstrate the use of these tools, the international benchmark of the OC4-DeepCwind platform is considered as a case study. The influence of the vessel mean position and design parameters in the stiffness, natural periods and oscillation modes is studied, revealing interesting coupling effects. Results are benchmarked against the commercial code OrcaFlex^{TM} showing good agreement, observing that the analytical result requires much less computational cost.

1. Introduction

Mooring system design is of vital importance for offshore floating systems. Not only operational requirements, but also financial demands can impact the whole design process. The mooring system must be both able to keep the vessel position within certain limits and cost-effective. This cost-efficiency is even more relevant in the floating offshore energy scenario than in the regular offshore Oil and Gas (O&G) industry. Indeed, offshore renewable energy projects are highly cost-sensitive and any over-design may compromise its feasibility. On the other hand, seeking for an optimal mooring system using high-order hierarchical models can be really expensive from the computational point-of-view. Such an aspect, together with deeper physical insights that can be gained, justifies efforts for analytical and expedite tools for design and analysis, mainly regarding initial phases of the project.

The design of a mooring system involves several parameters, such as: number, orientation, pretension and mechanical properties of mooring lines, geometric arrangement of the system, among others. In addition, the novel offshore renewable energy starts to attract investments and new conceptual studies have been being developed, resulting in different mooring technology and arrangements. For the sake of an example, [1] studied the effect of different line profiles on the response of a Floating Offshore Wind Turbine (FOWT) installed in shallow waters. The great complexity of such problems calls for a more basic understanding of the effects of the parameters on the response of the system. The use of analytical models can help to meet the demand, instead of the high number of computational simulations that might increase design cost.

* Corresponding author.
E-mail address: giovanni.amaral@usp.br (G.A. Amaral).

https://doi.org/10.1016/j.marstruc.2022.103189
Received 6 August 2021; Received in revised form 18 October 2021; Accepted 15 February 2022
Available online 9 March 2022

The mooring system stiffness matrix is a relevant information for any successful offshore floating structure project. The stiffness coefficients are of great value not only at the initial stages of design but also during verification and operational phases. For instance, the knowledge of the mooring stiffness matrix is mandatory, whenever slow-drift motions are concerned, being them the classical ones on the horizontal plane (surge, sway, yaw) or even those that might occur in heaving, pitching and rolling motions. As well known, slow-drift motions are resonant responses of the system at their low natural frequencies to the action of second-order wave forces in low frequencies, as well as to the action of wind forces or even current induced forces, and for which the mooring stiffness plays an important role. The mooring stiffness matrix may also have some influence in calculating the motion response of the vessel – complex (amplitude and phase) frequency responses – to first-order wave forces, commonly named as RAOs (Response Amplitude Operators).

The mooring system rule from BV [2] brings the requirements for the classification of the mooring system of floating units among others. According to the standard, the 6×6 stiffness matrix associates elementary displacements applied to the floating unit with the elementary reaction loads resulted from them, around a given position. Considering this, many authors have proposed different ways to evaluate the mooring system stiffness matrix.

Some authors were interested in specific applications and modeled only some portions of the stiffness matrix. [3] have proposed an analytical stiffness matrix formulation considering planar displacements on the vertical plane, for a given hydrostatic equilibrium condition, where the coordinates of the center of gravity were known *a priori*. Based on Taylor expansions techniques, [4] proposed an analytical formulation for the stiffness matrix of a generic mooring system, taking into account pretensioning effects of the mooring lines, however restricted to the unloaded equilibrium configuration. [5] [Chapter 8, page 265] presented a simple analytical formulation for the mooring system stiffness matrix, considering horizontal motions around the trivial equilibrium configuration, but without taking into account the effects of the mooring line pretensioning. [6] formulated the analytical mooring stiffness matrix for vertical planar motions, for a two-line mooring system. [7] proposed an analytical 3×3 stiffness matrix considering linear springs for the two-dimensional motions on the vertical plane. [8] numerically calculated, via Finite Element Method (FEM), the stiffness coefficients associated with translational motions, only. Recently, [9] presented a closed analytical formulation for the 3×3 stiffness matrix for the horizontal plane problem considering a generic heading and offset position of the vessel, by using Analytical Mechanics approaches.

Considering a full 6×6 stiffness matrix, [10] presented an analytical formulation around the trivial equilibrium position based on perturbation methods. In turn, [11] obtained the stiffness matrix by applying prescribed static offset analysis on a FEM model. In [12], the mooring system stiffness is numerically calculated with a linearization analysis around the mean equilibrium position of the platform using the results of the generalized forces *versus* displacements curves. Similarly to [10,13] formulated an analytical 6×6 stiffness matrix from perturbation methods, considering particular profiles for the mooring line.

The present paper proposes a closed-form analytical tool to assess the mooring system stiffness around any pre-stated position of the floating body, given the mooring line characteristic tension functions. It differs from [10] and from [13] numerical procedures, as the present formulation is based on classic methods of Analytical Mechanics, extending the derivation given in [9], instead of dealing with perturbation approaches. In addition, the presented formulation is not restricted to specific mooring line profiles. In other words, the formulation herein proposed is generic concerning the floating body geometry, position and mooring system parameters, including line profile. With this approach, the matrix is defined in a formal way, allowing to state some strong conclusions about motion couplings and symmetries. Determining the stiffness matrix at any given equilibrium position can be of particular interest for systems highly sensitive to offsets and attitude angles effects, such as FOWTs. [14,15] show that the mean horizontal offset and trim angle of the floater may potentially change the dynamic responses. By using the analytical formulation presented in [9,16] shows that the susceptibility of a multi-column semi-submersible to Vortex Induced Motions (VIM) can be highly dependent on the change of mooring stiffness due to offset variations. Experimental studies, including parametric ones, also may require a proper mooring stiffness matrix formulation for both, calibrating the mooring parameters and for numerical modeling of the physical results [15,17–20]. Finally, studies regarding the stability of the equilibrium position can be assessed by the analytical formulation of the stiffness matrix around given equilibrium points. Sensitivity studies herein developed by means of the analytical formulation are also another contribution of this paper. In this sense, the present paper is an extension of [9], to the full 3D case. This analytical tool is meant to help the design and analysis of mooring systems.

In order to present an application of the proposed methodologies, the OC4-DeepCwind semi-submersible platform is taken as case study. The stiffness coefficients are calculated for different offset scenarios, demonstrating the importance of a proper formulation. The effect of the heading angle on the coupling of the generalized coordinates is also investigated. The results are presented in the same innovative manner introduced in [9], by using colormaps for the stiffness matrix coefficients, plotted as function of offset position. These maps could help to understand the effects of the static vessel mean position on the mooring system stiffness. The use of the analytical formulation as a design tool is demonstrated by varying a parameter of the mooring line, namely the pretension.

The main contributions of this paper are: (i) a generic analytical formulation to compute the mooring system stiffness of a moored vessel and (ii) its use as a design and analysis tool. Due to the simplicity of the presented model, it can help mooring designers in basic understanding of the effects of the floating body position and mooring parameters on the stiffness parameters and natural periods of moored vessels.

For the sake of organization, the paper is structured as follows. The full closed-form analytical formulation of the mooring system stiffness matrix is derived in Section 2, the case study is developed in Section 3 and the conclusions are drawn in Section 4.

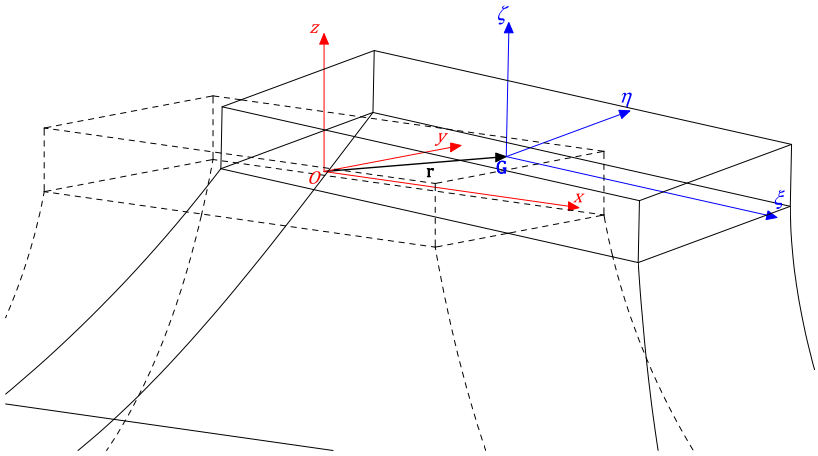

Fig. 1. Sketch of a generic floating body, moored by N mooring lines: at the equilibrium position of the autonomous system (dashed) and at a generic displacement position (full lines).

2. Stiffness matrix model

As already pointed out, the mooring system stiffness matrix is a key-point in the analysis of moored systems. In this context, the mooring forces that originally present nonlinear behavior should be linearized around any generic position of the floating body. The term "position of the floating body" is herein understood in a generic sense, as the formulation treats a 6-DOF problem. The term "trivial equilibrium position" is reserved to that for the externally unloaded system, i.e. under no current, wind or wave forces, nor any other external one, as a towing force applied by a tug boat, for instance. If constrained to motions on the horizontal plane, the term "generic position" may be interpreted as "offset" and "heading", regarding the trivial equilibrium one. By using classic Analytical Mechanics approaches, this section aims at presenting the mooring system stiffness matrix. The following is a three-dimensional extension of the planar formulation (horizontal plane) presented in [9].

2.1. Geometric relations

Fig. 1 schematically illustrates a floating body on a generic position, moored by N lines. Consider two reference frames: an inertial reference frame grounded on Earth O_{xyz} and a moving one and fixed to the body $G_{\xi\eta\zeta}$. Poles O and G are taken at the center of mass of the body at the trivial equilibrium position and at the displaced positions, respectively. These frames are defined by the orthonormal bases $E_x = (\hat{e}_x, \hat{e}_y, \hat{e}_z)$ and $E_\xi = (\hat{e}_\xi, \hat{e}_\eta, \hat{e}_\zeta)$.

The generalized coordinate vector considering all the vessel rigid motions is:

$$\mathbf{q} = [r_x \quad r_y \quad r_z \quad \phi \quad \theta \quad \psi]^t \tag{1}$$

where:

$$\mathbf{r} = [r_x \quad r_y \quad r_z]^t \tag{2}$$

are the three translational displacements[1] of $G_{\xi\eta\zeta}$ with respect to O_{xyz} and:

$$\boldsymbol{\theta} = [\phi \quad \theta \quad \psi]^t \tag{3}$$

are three rotation angles, defined following the Ocean Engineering order[2]. These angles define the rotation matrix between the reference frames, $[\mathbb{R}]_{E_x|E_\xi}$. This rotation matrix is given in Appendix.

The position of a fairlead $P^{(i)}$ with respect to G and given in the moving frame is:

$$\overline{P}^{(i)}_{E_\xi} = \left(P^{(i)} - G\right) = \left[p^{(i)}_\xi \quad p^{(i)}_\eta \quad p^{(i)}_\zeta\right]^t \tag{4}$$

On the other hand, the fairlead position $P^{(i)}$ with respect to the origin O and represented in the grounded reference frame is:

$$\overline{P}^{(i)}_{E_x} = \left(P^{(i)} - O\right) = \left[p^{(i)}_x \quad p^{(i)}_y \quad p^{(i)}_z\right]^t = \mathbf{r} + [\mathbb{R}]_{E_x|E_\xi}\overline{P}^{(i)}_{E_\xi} \tag{5}$$

[1] The components of $\mathbf{r}$ are written with respect to the fixed reference frame. One should not confuse these displacements with classical Ocean Engineering surge, sway and heave motions, all those defined in a frame that follows the body (not necessarily the body frame), having one local cartesian axis vertical and the other two horizontal.

[2] First the rotation in yaw ψ direction, followed by a rotation in pitch θ and, finally, a rotation in roll ϕ.

Accordingly, the position of an anchor $A^{(i)}$ in the grounded reference frame is:

$$\overrightarrow{A}^{(i)}_{E_x} = \left(A^{(i)} - O\right) = \begin{bmatrix} a_x^{(i)} & a_y^{(i)} & a_z^{(i)} \end{bmatrix}^t \tag{6}$$

In this context, the horizontal and vertical projections of the anchor–fairlead distance ($h_f^{(i)}$ and $v_f^{(i)}$, respectively) are determined as:

$$h_f^{(i)} = \sqrt{\left(a_x^{(i)} - p_x^{(i)}\right)^2 + \left(a_y^{(i)} - p_y^{(i)}\right)^2} \tag{7}$$

$$v_f^{(i)} = p_z^{(i)} - a_z^{(i)} \tag{8}$$

Both projections follow directions that can be written with respect to the fixed reference frame, by defining unity directional vectors $\hat{e}_h^{(i)}$ and $\hat{e}_v^{(i)}$. These vectors are defined from the fairlead to the anchor, as follows:

$$\hat{e}_h^{(i)} = \cos\alpha^{(i)}\hat{e}_x + \sin\alpha^{(i)}\hat{e}_y \tag{9}$$

$$\hat{e}_v^{(i)} = -\hat{e}_z \tag{10}$$

where:

$$\cos\alpha^{(i)} = \frac{a_x^{(i)} - p_x^{(i)}}{r^{(i)}} \tag{11}$$

$$\sin\alpha^{(i)} = \frac{a_y^{(i)} - p_y^{(i)}}{r^{(i)}} \tag{12}$$

Finally, it is important to notice that $h_f^{(i)}$, $v_f^{(i)}$, $\hat{e}_h^{(i)}$, $\hat{e}_v^{(i)}$ and $\alpha^{(i)}$ are functions of the generalized coordinates, since they depend on the position of the fairleads with respect to the fixed frame, $\overrightarrow{P}^{(i)}_{E_x}$.

2.2. Generalized restoring mooring forces

This subsection brings a closed-form analytical formulation for the generalized restoring forces due to the mooring lines. It is worth to be emphasized, though, that in this model the mooring system is supposed to be conservative, i.e., no sort of non-conservative forces is considered acting on the lines, as current drag forces or friction ones that may be imposed in the contact with the soil. Therefore, the mooring lines are supposed to be subjected only to gravity and to elastic effects due to extensibility of the line, besides reaction forces applied to their extremities, fairleads and anchors, here considered as holonomic constraints. In summary, the system is considered conservative, mooring lines remaining in vertical planes. It is also worth mentioning that, besides being of extreme importance for design applications and analysis, the present model does not consider the dynamics of the mooring lines and may be considered quasi-static in this sense.

Based on those simplifying assumptions, the tension of each mooring line at the fairlead may be written as function of $h_f^{(i)}$ and $v_f^{(i)}$, the so-called characteristic tension curve. For the present formulation, any possible mooring line configuration can be used. However, it is important to highlight that these characteristic functions should be known *a priori*, respecting the strong hypothesis that they must be function of the relative anchor–fairlead distances, only. For classic inextensible and extensible catenary lines, the analytical formulations are well known; see, for instance, [5]. In cases where the analytical formulation is not known, high-hierarchy models, such as those based on the FEM, might be used. Using the directional vectors $\hat{e}_h^{(i)}$ and $\hat{e}_v^{(i)}$, defined in Eqs. (9) and (10), the tension vector force at the fairlead can be written as follows:

$$\overrightarrow{T}^{(i)}(h_f^{(i)}, v_f^{(i)}) = F_H^{(i)}(h_f^{(i)}, v_f^{(i)})\hat{e}_h^{(i)} + F_V^{(i)}(h_f^{(i)}, v_f^{(i)})\hat{e}_v^{(i)} \tag{13}$$

$F_H^{(i)}$ and $F_V^{(i)}$ being the horizontal and vertical forces for the ith mooring line.

Considering the effect of each mooring line at the vessel, the generalized restoring mooring force vector can be defined correspondingly to the generalized coordinate vector $\mathbf{q}$.

$$\mathbf{Q} = \begin{bmatrix} Q_{r_x} & Q_{r_y} & Q_{r_z} & Q_\phi & Q_\theta & Q_\psi \end{bmatrix}^t \tag{14}$$

Then, from Analytical Mechanics (see, for example, [21]):

$$Q_j = \sum_{i=1}^{N} Q_j^{(i)} = \sum_{i=1}^{N} \overrightarrow{T^{(i)}} \cdot \frac{\partial \overrightarrow{P}^{(i)}}{\partial q_j} = \sum_{i=1}^{N} \left(F_H^{(i)}\hat{e}_h^{(i)} + F_V^{(i)}\hat{e}_v^{(i)}\right) \cdot \frac{\partial \overrightarrow{P}^{(i)}}{\partial q_j} \tag{15}$$

where $Q_j^{(i)}$ is the jth generalized restoring force associated with the ith line.

After some algebraic work (see [22]), one may find that the components of $Q^{(i)}$ are:

$$Q_{r_x}^{(i)} = F_H^{(i)}\cos\alpha^{(i)} \tag{16}$$

$$Q_{r_y}^{(i)} = F_H^{(i)}\sin\alpha^{(i)} \tag{17}$$

$$Q_{r_z}^{(i)} = -F_V^{(i)} \tag{18}$$

$$Q_{\phi}^{(i)} = F_H^{(i)} \left(\cos\alpha^{(i)} \frac{\partial p_x^{(i)}}{\partial \phi} + \sin\alpha^{(i)} \frac{\partial p_y^{(i)}}{\partial \phi} \right) - F_V^{(i)} \frac{\partial p_z^{(i)}}{\partial \phi} \tag{19}$$

$$Q_{\theta}^{(i)} = F_H^{(i)} \left(\cos\alpha^{(i)} \frac{\partial p_x^{(i)}}{\partial \theta} + \sin\alpha^{(i)} \frac{\partial p_y^{(i)}}{\partial \theta} \right) - F_V^{(i)} \frac{\partial p_z^{(i)}}{\partial \theta} \tag{20}$$

$$Q_{\psi}^{(i)} = F_H^{(i)} \left(\cos\alpha^{(i)} \frac{\partial p_x^{(i)}}{\partial \psi} + \sin\alpha^{(i)} \frac{\partial p_y^{(i)}}{\partial \psi} \right) \tag{21}$$

2.3. Mooring system stiffness matrix

The generalized forces presented in the previous section are dependent on position only and, therefore, can be seen as potential forces, i.e. forces arisen from a potential function.

$$Q_j = -\frac{\partial V}{\partial q_j} \tag{22}$$

where:

$V = V(\mathbf{q}, \Pi)$ is the potential energy, and

$\Pi = \left\{ \left(A^{(i)}, P^{(i)}, F_H^{(i)}, F_V^{(i)} \right) \middle| i = 1, \ldots, N \right\}$ is the set of parametric functions of the mooring system.

Then, locally, around any generic position $\mathbf{q}^0$, the mooring system stiffness matrix $[\mathbb{K}](\mathbf{q}^0)$ may be defined as the Hessian matrix of $V(\mathbf{q}, \Pi)$ at that point:

$$\mathbb{K}(\mathbf{q}^0) = \left[\frac{\partial^2 V}{\partial q_j \partial q_k} \right]_{\mathbf{q}^0} = - \left[\frac{\partial Q_j}{\partial q_k} \right]_{\mathbf{q}^0} \tag{23}$$

Considering the definition of the generalized forces from Eq. (15) and recalling that $F_H^{(i)}$, $F_V^{(i)}$, $\hat{e}_h^{(i)}$ and $\hat{e}_v^{(i)}$ are functions of $\mathbf{q}$, after some algebra, each component of the 6×6 stiffness matrix associated with the mooring system can be written as:

$$\begin{aligned} K_{jk} = \sum_{i=1}^{N} K_{jk}^{(i)} = &- \sum_{i=1}^{N} \left(\frac{\partial F_H^{(i)}}{\partial h_f^{(i)}} \frac{\partial h_f^{(i)}}{\partial q_k} + \frac{\partial F_H^{(i)}}{\partial v_f^{(i)}} \frac{\partial v_f^{(i)}}{\partial q_k} \right) \hat{e}_h^{(i)} \cdot \frac{\partial \overrightarrow{P}^{(i)}}{\partial q_j} + \\ &- \sum_{i=1}^{N} \left(\frac{\partial F_V^{(i)}}{\partial h_f^{(i)}} \frac{\partial h_f^{(i)}}{\partial q_k} + \frac{\partial F_V^{(i)}}{\partial v_f^{(i)}} \frac{\partial v_f^{(i)}}{\partial q_k} \right) \hat{e}_v^{(i)} \cdot \frac{\partial \overrightarrow{P}^{(i)}}{\partial q_j} + \\ &- \sum_{i=1}^{N} \left[F_H^{(i)} \frac{\partial}{\partial q_k} \left(\hat{e}_h^{(i)} \cdot \frac{\partial \overrightarrow{P}^{(i)}}{\partial q_j} \right) + F_V^{(i)} \frac{\partial}{\partial q_k} \left(\hat{e}_v^{(i)} \cdot \frac{\partial \overrightarrow{P}^{(i)}}{\partial q_j} \right) \right] \end{aligned} \tag{24}$$

with $K_{jk}^{(i)}$ being the stiffness coefficient for the ith mooring line.

Notice that $\mathbf{q}^0$ is considered given and represents an arbitrary position of the system, possibly under the action of steady constant forces. All coefficients in Eq. (24) are fully developed in Appendix.

Some interesting points should be highlighted here. Firstly, as expected, the resulting stiffness matrix is symmetric, provided the considered forces are purely conservative. Indeed, as it can be seen from the fully developed coefficients in Appendix, coefficients $K_{jk} = K_{kj}$ as $\partial F_H^{(i)} / \partial v_f^{(i)} = \partial F_V^{(i)} / \partial h_f^{(i)}$. In addition, it is crucial to understand that the given stiffness matrix is not defined at the moving frame E_{ξ}. In other words, it is not defined with respect to the frame fixed to the body. If the reader intents to work on this reference frame, one should rotate the result. This operation is shown in Appendix.

Regarding the expressions for the stiffness coefficients, it is noticeable that some are combinations of others. This allows to rewrite the stiffness matrix in a more elegant and concise way. Consider the partitions of the matrix, by representing only the translational DOF as $\mathbb{K}_{TT}^{(i)}$. The partition representing the coupling between translational and rotational motions is $\mathbb{K}_{TR}^{(i)}$ and the one associated with the rotational DOF only as $\mathbb{K}_{RR}^{(i)}$. As the stiffness matrix is symmetric, $\mathbb{K}_{RT}^{(i)} = \mathbb{K}_{TR}^{(i)^t}$. Then, the stiffness matrix associated with the ith mooring line can be expressed as:

$$\mathbb{K}^{(i)} = \left(\begin{array}{c|c} \mathbb{K}_{TT}^{(i)} & \mathbb{K}_{TR}^{(i)} \\ \hline \mathbb{K}_{TR}^{(i)} & \mathbb{K}_{RR}^{(i)} \end{array} \right) \tag{25}$$

Considering coefficients from partition $\mathbb{K}_{TR}^{(i)}$, it is possible – as showed in the respective equations – to rewrite them as:

$$\mathbb{K}_{TR}^{(i)} = \mathbb{K}_{TT}^{(i)} \cdot \boldsymbol{\nabla} \left([\mathbb{R}]_{E_x | E_{\xi}} \cdot \overrightarrow{P^{(i)}}_{E_{\xi}} \right) \tag{26}$$

with:

$$\boldsymbol{\nabla}[\quad](\phi, \theta, \psi) = \left(\frac{\partial[\quad]}{\partial \phi}, \frac{\partial[\quad]}{\partial \theta}, \frac{\partial[\quad]}{\partial \psi} \right) \tag{27}$$

Now, we focus on the partition $[\mathbb{K}_{RR}]$. From the aforementioned coefficients:

$$\mathbb{K}_{RR}^{(i)} = \mathbb{K}_{RR}^{(i)*} - \bar{\mathbb{K}}_{RR}^{(i)} \tag{28}$$

with:

$$\mathbb{K}_{RR}^{(i)*} = \boldsymbol{\nabla}^t \left(\mathbb{R}_{E_x|E_\xi} \cdot \overrightarrow{P^{(i)}}_{E_\xi} \right) \cdot \mathbb{K}_{TR}^{(i)} \tag{29}$$

and

$$\bar{\mathbb{K}}_{RR}^{(i)} = \frac{\partial^2 p_x^{(i)}}{\partial \boldsymbol{\theta}^2} F_H^{(i)} \cos\alpha^{(i)} + \frac{\partial^2 p_y^{(i)}}{\partial \boldsymbol{\theta}^2} F_H^{(i)} \sin\alpha^{(i)} - \frac{\partial^2 p_z^{(i)}}{\partial \boldsymbol{\theta}^2} F_V^{(i)} \tag{30}$$

recalling that $\boldsymbol{\theta} = [\phi \quad \theta \quad \psi]^t$.

Thus, the stiffness coefficients associated with the translation–rotation and rotation only motions are functions of the stiffness coefficients associated with the translational DOFs. In fact, by only defining the stiffness coefficients of the translational motions, one may find all the others only by geometry.

As a particular but important case, let us consider a perfectly polar symmetry for the mooring system. A polar symmetry is herein defined by taking a vertical axis passing through the pole G, in the unloaded condition, with all fairleads equidistant to it and all mooring line planes intercepting this very axis. A good image for this picture is a regular polygonal arrangement. This is the case of the OC4 platform, studied in Section 3; see Fig. 3(a). In this scenario, it is possible to show that the only non-null mooring stiffness coefficients for a N-line symmetric arrangement become:

$$K_{11} = \frac{n}{2}(k_{HH} + \bar{k}_{HH}) \tag{31}$$

$$K_{15} = K_{51} = \frac{n}{2}(k_{VH} l + k_{HH} p_\zeta + \bar{k}_{HH} p_\zeta) \tag{32}$$

$$K_{22} = \frac{n}{2}(k_{HH} + \bar{k}_{HH}) \tag{33}$$

$$K_{24} = K_{42} = -\frac{n}{2}(k_{VH} l + k_{HH} p_\zeta + \bar{k}_{HH} p_\zeta) \tag{34}$$

$$K_{33} = n k_{VV} \tag{35}$$

$$K_{44} = \frac{n}{2}(p_\zeta^2 k_{HH} + p_\zeta^2 \bar{k}_{HH} + 2 p_\zeta l k_{HV} + l^2 k_{VV} + l F_H - 2 p_\zeta F_V) \tag{36}$$

$$K_{55} = \frac{n}{2}(p_\zeta^2 k_{HH} + p_\zeta^2 \bar{k}_{HH} + 2 p_\zeta l k_{HV} + l^2 k_{VV} + l F_H - 2 p_\zeta F_V) \tag{37}$$

$$K_{66} = n \bar{k}_{HH} l^2 \left(1 - \frac{h}{l}\right) \tag{38}$$

where l is the radius from the platform vertical central line to the fairleads, $k_{HH} = \left[\frac{\partial F_H}{\partial h_f}\right]_{\mathbf{q}^0}$, $k_{VV} = \left[\frac{\partial F_V}{\partial v_f}\right]_{\mathbf{q}^0}$ and $k_{HV} = \left[\frac{\partial F_H}{\partial v_f}\right]_{\mathbf{q}^0}$ are the horizontal, vertical and coupled local stiffness and $\bar{k}_{HH} = \frac{F_H(h_f^0, v_f^0)}{h_f^0}$ is the so called horizontal "string stiffness", relevant for some mooring system arrangements including symmetric ones; see [9].

The mooring system stiffness enables multiple applications. Considering the planar motions ($[r_x \quad r_y \quad \psi]^t$), it is possible to evaluate the natural periods and the equivalent modes of oscillation by simply solving the corresponding linear eigenvalue problem. This can be done for the motions on the horizontal plane only, by taking the asymptotic limit at zero frequency for the values of their respective added mass coefficients. In this scenario, the corresponding 3×3 stiffness matrix recovers the one obtained in [9]. Section 3 brings discussions of this linear eigenvalue problem in the context of a case study. The periods will also be functions of the mean equilibrium position and heading. In this context, the presented formulation can be used to analyze resonant responses for a vessel that, under the concomitant action of other static loads, has a non-trivial equilibrium position. Thus, this tool can help to desynchronize the natural periods (to each other, thus avoiding internal resonances as well as from the environmental loads periods, avoiding forced resonance behaviors) not only in the trivial position but at typical mean equilibrium ones. For instance, [16] applied this formulation to investigate the susceptibility of a multi-column semi-submersible platform to VIM, for a whole turn of sea current incidences and different velocities — resulting in different equilibrium position, comparing with reduced order phenomenological models and experimental results. This analytical formulation can also be helpful when comparing different concepts in an optimization schemes. The mooring system stability can also be studied from the analytical model. For example, Eq. (79) shows that the yaw stiffness coefficient is function of the fairlead radius. Reducing the fairlead radius may lead to loss of stability in heading.

On the other hand, considering all six DOF, the classic RAOs and their respective phases might be assessed, once the added mass tensor and the first-order wave forces (amplitude and phase) are considered determined, as functions of frequency, from any seakeeping potential flow code. This can be done for any given equilibrium position and attitude (heading, trim and heel) of the floating unit, at which the mooring stiffness matrix is obtained with the present formulation. The resulting stiffness matrix may contribute for dynamic couplings (surge-heave-pitch, for instance), as presented by [15].

The formulation herein proposed can also be seen as both design and operational tool, as it helps to easily investigate the influence of line parameters on the stiffness and natural periods of the whole system. Thus, designers can set specific thresholds and vary the parameters in order to find the best initial mooring concepts for analysis using more time-consuming higher-order hierarchical models (FEM, for example). During operation, the closed form formulation allows active winch performances to change natural periods by varying the mooring length and pretension, for instance. Next section brings a case study that illustrates this design/operation parameter analysis.

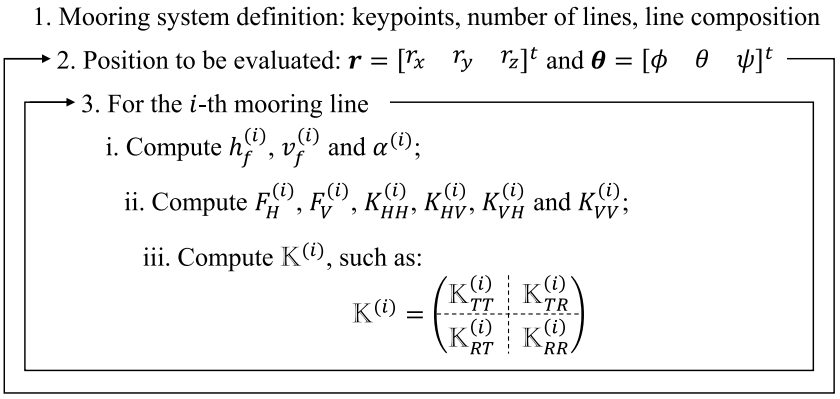

Fig. 2. Step-by-step procedure for the mooring system stiffness calculation.

Table 1
The OC4-DeepCwind original mooring system parameters.

Number of mooring lines	3
System type	Spread system
Line profile	One-segment
Line composition	Chain
Water depth	200 m
Fairlead depth	14 m
Radius from center to anchors	834.6 m
Radius from center to fairleads	40.9 m
Unstretched length	835.35 m
Mass per unit length	113.35 kg/m
Equivalent diameter	76.6 mm
Axial Stiffness	753.6 MN

Before addressing the case studies themselves, Fig. 2 brings the step-by-step procedure for evaluating the stiffness matrix using the formulation herein proposed. In the figure, keypoints denote the position of the mooring lines anchors and fairleads, with respect to the global and local references frames, respectively. The second step can be used in a recursive way, allowing the user to plot the colormaps (as it is presented later in this paper), or just once, to evaluate the stiffness matrix at a specific position (being the trivial equilibrium position or not). Then, for each mooring line, the horizontal, $h_f^{(i)}$, and vertical, $v_f^{(i)}$, projections of the fairlead-anchor distance need to be calculated, as well as the "attacking" angle, $\alpha^{(i)}$. From the characteristic tension functions[3] ($F_H^{(i)}(h_f^{(i)}, v_f^{(i)})$ and $F_V^{(i)}(h_f^{(i)}, v_f^{(i)})$), the components of the tension at the fairlead ($F_H^{(i)}$ and $F_V^{(i)}$) and their derivatives ($K_{HH}^{(i)}$, $K_{HV}^{(i)}$, $K_{VH}^{(i)}$ and $K_{VV}^{(i)}$) can be easily assessed. Finally, the resulting stiffness matrix is computed by applying Eq. (44) to (79).

3. Case studies

Aiming at illustrating and discussing the application of the analytical method herein proposed, the OC4-DeepCwind semi-submersible Floating Offshore Wind Turbine (FOWT) [12] is taken as a case study. The stiffness matrix and horizontal plane natural periods for the trivial equilibrium position is compared with literature results [12]. The influence of mooring pretension is also investigated, demonstrating the use of the analytical tool in design/operations phases. The importance of defining the matrix for an equilibrium position other than the trivial one is also discussed through an interesting use of the presented tool, plotting colored maps of the stiffness coefficients as functions of the offset r_x and r_y. This follows an innovative way to display the results, originally proposed in [9]. The linear eigenvalue problem is solved for the motions on the horizontal plane, allowing to determine the natural periods and their respective oscillation modes. Colormaps for the natural periods are also included. The stiffness matrix colorplot is then compared with numerical result obtained using Orcaflex™ [23].

The original OC4-DeepCwind mooring arrangement proposed by [12] is an equidistant 3 × 1 spread mooring system. Fig. 3(a) shows the top view of the original design system. The mooring line profile is an one-segment mooring chain. Fig. 3(b) depicts the mooring line profile and Table 1 presents its parameters.

[3] It is important to highlight again that for computing the ith mooring line contribution for the whole system stiffness matrix, the characteristic tension functions have to be known *a priori*, seen as inputs of the present problem. Again, for some cases, such as catenary-laying, the analytical formulation is known. When not, the characteristic tension functions might be determined using numerical methods, e.g. FEM modeling.

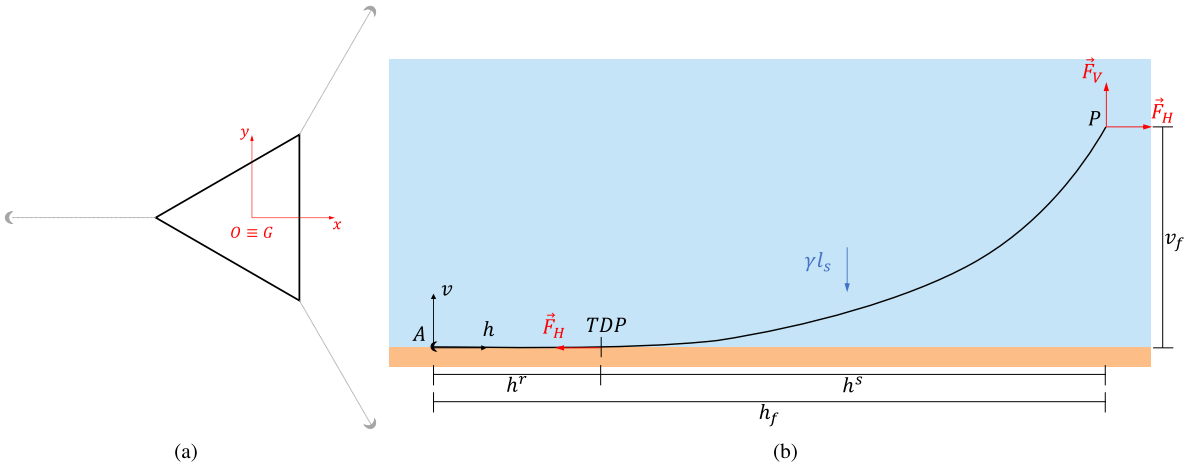

Fig. 3. The OC4-DeepCwind floating wind original mooring system: (a) Top view and (b) Chain mooring line profile.

Table 2
The OC4-DeepCwind original mooring line forces and stiffness.

Pretensioning (f_{OC4})	1.16E+3 kN
Horizontal force (F_H)	9.63E+2 kN
Vertical force (F_V)	6.49E+2 kN
Horizontal local stiffness (k_{HH})	5.29E+1 kN/m
Vertical local stiffness (k_{VV})	6.84 kN/m
Coupled local stiffness (k_{HV})	1.62E+1 kN/m
Horizontal "string stiffness" ($\bar{k}_{HH}$)	1.21 kN/m

As aforementioned, for the one-segment mooring line, the characteristic tension curves are known extensible catenary equations, with γ and EA being the immersed weight per unit length and the axial stiffness, respectively (see, for instance [5]):

$$h_f = l - \frac{1}{\gamma}F_V + \frac{F_H}{EA}l + \frac{F_H}{\gamma}\ln\left(\frac{F_V + \sqrt{F_H^2 + F_V^2}}{F_H}\right) \tag{39}$$

$$v_f = \frac{1}{\gamma}\sqrt{F_H^2 + F_V^2} + \frac{1}{2}\frac{F_V^2}{EA\gamma} \tag{40}$$

Again, notice that Eqs. (39) and (40) are written in the inverted form, i.e. the distances as function of the forces at the fairlead. For the development herein proposed, it is necessary to numerically evaluate forces as well a tangent stiffness (in the plane of the line) and "string" stiffness (normal to the plane). This can be done by using the Newton–Raphson method for instance. Table 2 brings the stiffness values for the trivial equilibrium position.

The mooring system stiffness $[\mathbb{K}]_A$ for the trivial equilibrium position, obtained from the methodology herein proposed, is then presented in Eq. (values in kN, m and rad). The obtained results are in agreement with those from [12], presented in Eq. (42).

$$[\mathbb{K}]_A = \begin{pmatrix} 7.09\text{E+1} & 0 & 0 & 0 & -1.07\text{E+2} & 0 \\ 0 & 7.09\text{E+1} & 0 & 1.07\text{E+2} & 0 & 0 \\ 0 & 0 & 1.91\text{E+1} & 0 & 0 & 0 \\ 0 & 1.07\text{E+2} & 0 & 8.73\text{E+4} & 0 & 0 \\ -1.07\text{E+2} & 0 & 0 & 0 & 8.73\text{E+4} & 0 \\ 0 & 0 & 0 & 0 & 0 & 1.17\text{E+5} \end{pmatrix} \tag{41}$$

$$[\mathbb{K}]_N = \begin{pmatrix} 7.08\text{E+1} & 0 & 0 & 0 & -1.08\text{E+2} & 0 \\ 0 & 7.08\text{E+1} & 0 & 1.08\text{E+2} & 0 & 0 \\ 0 & 0 & 1.91\text{E+1} & 0 & 0 & 0 \\ 0 & 1.07\text{E+2} & 0 & 8.73\text{E+4} & 0 & 0 \\ -1.07\text{E+2} & 0 & 0 & 0 & 8.73\text{E+4} & 0 \\ 0 & 0 & 0 & 0 & 0 & 1.17\text{E+5} \end{pmatrix} \tag{42}$$

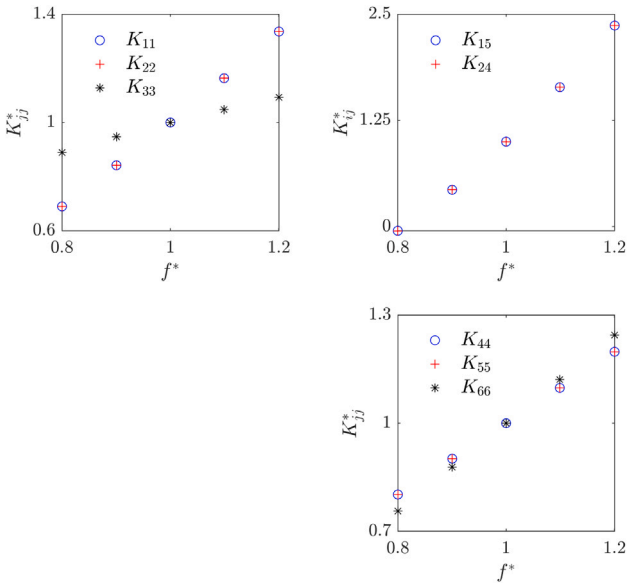

Fig. 4. Effect of the mooring line dimensionless pretension at the dimensionless stiffness coefficients.

Here, some important comments should be done. Firstly, note that the resulting matrix from the analytical methodology is symmetric, as expected from Section 2.3[4]. However, the result presented by [12] is a non symmetric stiffness matrix. The mooring model used by those authors considered non-conservative forces related to the friction of the mooring lines with the seabed, what may be the main reason for the non-symmetry of the resulting matrix. Another explanation for the difference come from the resolution required for the numerical method used by [12]. In fact, in that paper, the stiffness coefficients were calculated via central-differences of the force–displacement curves. Those curves were obtained by imposing small perturbations around the trivial equilibrium position in all six DOFs, resulting in restoring forces. Thus, the final result is sensitive to the approximation considered for the small perturbations. This indicates an interesting gain of the analytical model, as it is evaluated with precision. In other words, one may consider the analytical stiffness matrix herein proposed as the "tangential" stiffness matrix, and the one found through prescribed perturbations as the "secant" matrix. Additionally, while the prescribed static offsets analysis via central-differences needs to evaluate the forces in 18 distinguish points (three points for each degree of freedom), the analytical formulation requires the computation of lines' forces and stiffness at one point only, which can be interesting for successive evaluations.

The formulation allows to investigate the effects of varying line parameters on the system stiffness in a easy way. Fig. 4 brings the influence of the variations of the line pretension on the stiffness coefficients. The values are dimensionless with respect to the OC4 base case (i.e. $f^* = f/f_{OC4}$ and $K^*_{ij} = K_{ij}/K_{ij_{OC4}}$). It is remarkable that the coefficients vary differently. This could help design and operation decisions in terms of stiffness requirements and natural periods, for instance. The pretension is function of the nominal length of the mooring line, allowing to establish a relation between line length (and, consequently, acquisition costs), stiffness and tension.

As pointed out, an important gain from the methodology is to evaluate the mooring system stiffness at different mean positions. For instance, let us consider that the mean equilibrium position of the vessel is no longer the trivial one but at an initial heading angle $\bar{\psi} = 5°$, caused by any static load, with all other generalized coordinates null. The stiffness matrix $[\mathbb{K}]_{\bar{\psi}}$ is presented in Eq. (43) (values in kN, m and rad).

$$[\mathbb{K}]_{\bar{\psi}} = \begin{pmatrix} 7.16E{+}1 & 0 & 0 & -9.14E{+}1 & -1.08E{+}2 & 0 \\ 0 & 7.16E{+}1 & 0 & 1.08E{+}2 & -9.14E{+}4 & 0 \\ 0 & 0 & 1.92E{+}1 & 0 & 0 & 1.63E{+}2 \\ -9.14E{+}1 & 1.08E{+}2 & 0 & 8.77E{+}4 & -5.14E{+}3 & 0 \\ -1.08E{+}2 & -9.14E{+}4 & 0 & -5.14E{+}3 & 8.77E{+}4 & 0 \\ 0 & 0 & 1.63E{+}2 & 0 & 0 & 1.19E{+}5 \end{pmatrix} \tag{43}$$

Notice that even for a small yaw rotation, some coefficients that are null at non-yawed condition, assume non-null values. Notice also that the matrix remains symmetric, resulting from the conservative mooring forces consideration. Features like those make closed-form formulations important for proper evaluations. Additionally, it is also possible to map the coefficients for different

[4] In fact, as only conservative forces are considered in the mooring line model, the stiffness matrix is nothing more than the Hessian of a scalar function V, a mooring force potential function, calculated at a given position. As well known, Hessian matrices are symmetric by construction, thanks to the linear properties of the partial derivative operators, which lead to their interchangeability and, therefore, to symmetry.

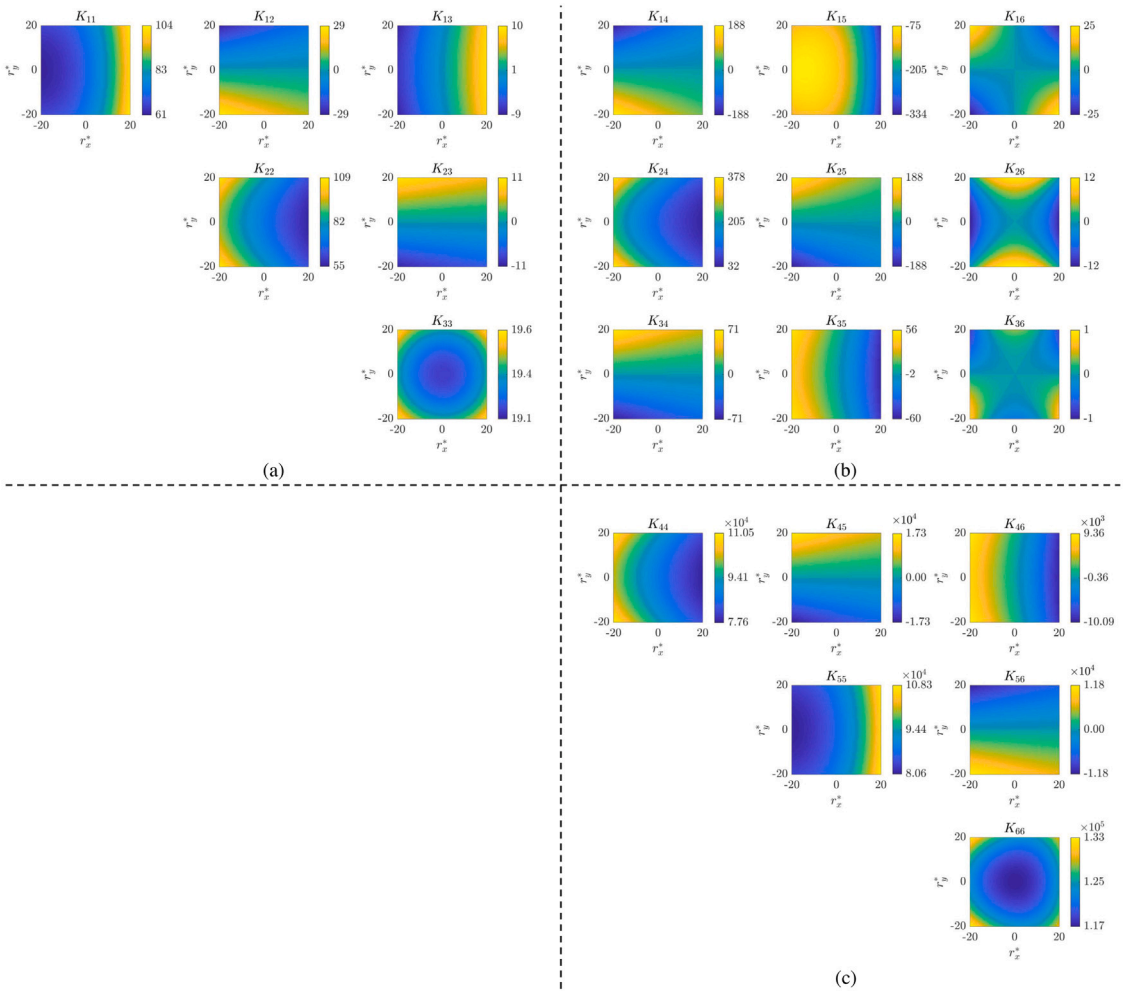

Fig. 5. Stiffness coefficients as function of the offset – OC4-DeepCwind all-chain mooring system: partitions (a) $\mathbb{K}_{TT}$ (unities: kN/m), (b) $\mathbb{K}_{TR}$ (unities: kN/rad) and (c) $\mathbb{K}_{RR}$ (unities: kNm/rad). Offset normalized. Immediate (three seconds) construction of the whole map, with an Intel™ core i7 quad core processor and 16 Gb of RAM.

offset positions, following the innovative strategy proposed in [9]. As an example, colored maps of the mooring system stiffness matrix coefficients are plotted as functions of the platform offset. This is done by varying parametrically the offset in the range $r_x^* = r_y^* = [-20\%R_f; 20\%R_f]$, being $[r_x^*, r_y^*] = [r_x/R_f, r_y/R_f]$, where R_f is the distance of the fairleads from the platform vertical central line passing through G. All other generalized coordinates are left unaltered and null. Fig. 5 brings these maps for the a 81×81 mesh, presenting the partitions $\mathbb{K}_{TT}$, $\mathbb{K}_{TR}$ and $\mathbb{K}_{RR}$. Notice that due to the symmetry of the stiffness matrix, only the upper-triangular matrix is shown.

The color maps can be analyzed as follows. Consider that a constant external load changes the equilibrium position from the trivial one to another. The mooring system stiffness coefficients must be recalculated. The methodology herein presented could help designers to rapidly evaluate and design the mooring system, taking into account the dependence of the stiffness matrix on the equilibrium position. Additionally, some stability studies, such as the use of catastrophe sets [24,25], can be also conducted by using this kind of maps, considering scenarios where the system might lose stiffness. The loss of stability can have different origins, such as variation in the mooring parameters, external forces magnitudes (and the consequent equilibrium position) among others. In other words, the analytical formulation herein proposed allows an easy investigation on the variation of the real and imaginary parts of the eigenvalues due to variations of the system parameters. Although a mooring system equilibrium stability study is of great relevance, it is kept for further works.

It is possible to compute similar colormaps using other methods to calculate the mooring system stiffness. However, this could be computationally inefficient, as it depends on the efficiency of computing the stiffness coefficients for each point of the map. For instance, the stiffness maps can be assessed by using numerical tools based on higher-order hierarchical models, such as OrcaFlex™ . This result is presented in Fig. 6, considering a 1000-element mesh for each line, for the same 81×81 map. It is clear that the results are in good agreement, showing consistency in the implementation of the codes. However, it matters emphasizing that OrcaFlex™

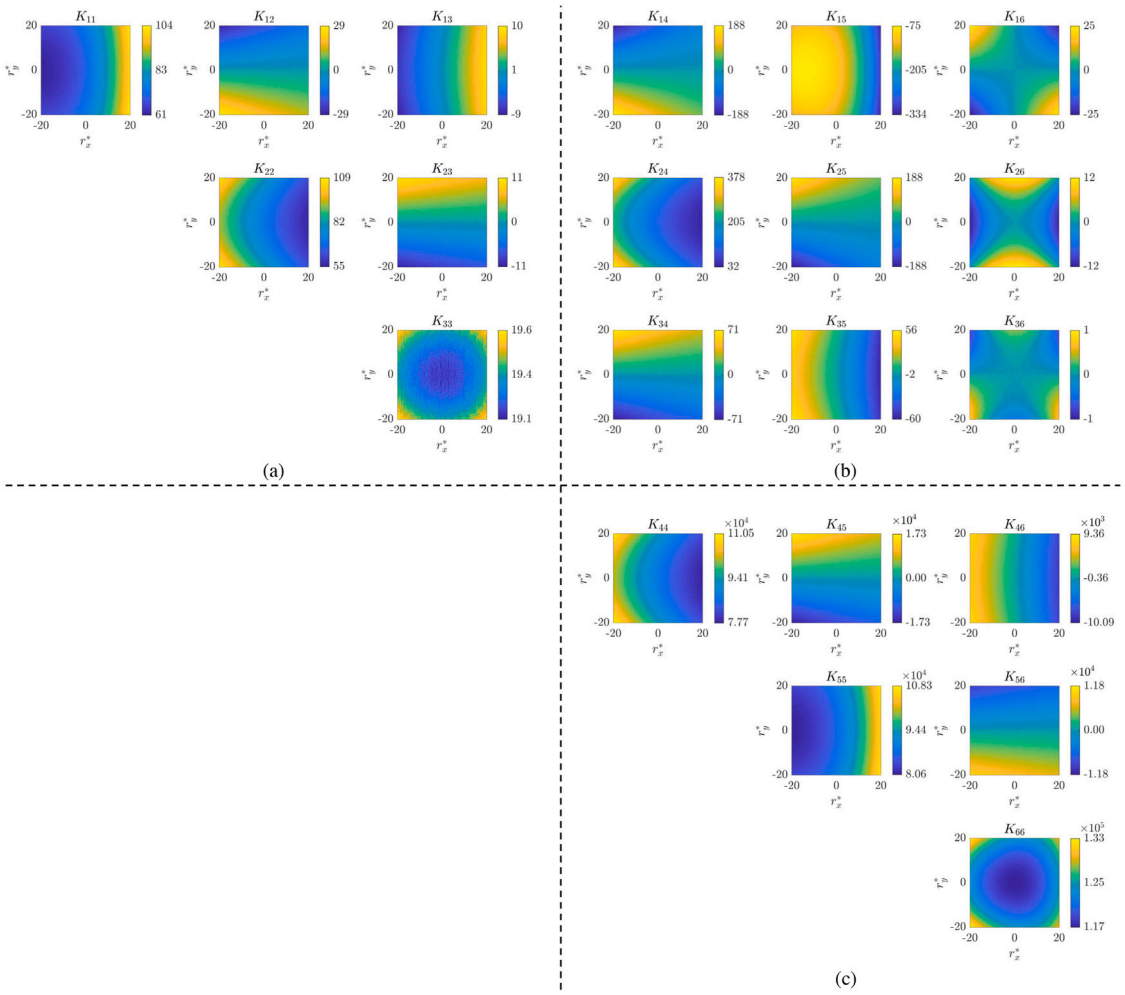

Fig. 6. Stiffness coefficients as function of the offset – OC4-DeepCwind all-chain mooring system obtained using OrcaFlex™ : partitions (a) $\mathbb{K}_{TT}$ (unities: kN/m), (b) $\mathbb{K}_{TR}$ (unities: kN/rad) and (c) $\mathbb{K}_{RR}$ (unities: kNm/rad). Offset normalized. Five hours to run the whole map, with an Intel™ core i7 quad core processor and 16 Gb of RAM.

coefficient K_{33} presents a small blur due to computational convergence, even for such discretized mesh. For low discretized meshes, other coefficients could also present blurred maps. In terms of computational efficiency, the latter takes over five hours to run the whole map, while the analytical result is obtained almost immediately (less than three seconds) using the same computer (an Intel™ core i7 quad core processor and 16 Gb of RAM). Such comparison can be helpful to evaluate codes and meshes, which, under the same hypothesis (conservative system), should recover the analytical result for every point. In fact, the analytical result can be used as the paradigm for mesh convergence analysis.

Regarding the maps, notice that the stiffness coefficients vary substantially, even if the offset is within operational limits. Additionally, some degrees of freedom that are not coupled at the trivial position might be coupled at a certain offset — see, for example, the stiffness coefficient K_{12}. This illustrates the influence of the system configuration on the mooring system stiffness, justifying the use of an analytical model for evaluations at that real equilibrium position, instead of taking into account the stiffness matrix at the trivial one.

Furthermore, one may see some anti-symmetric and symmetric patterns in the colored maps. For instance, notice the symmetry of the elements in the diagonal with the respect to the displacement r_y, as expected following the symmetry of the mooring system at the trivial position. Considering the planar DOFs, i.e. r_x, r_y and ψ, the symmetric/anti-symmetric pattern is even more pronounced. K_{12} is anti-symmetric with respect to r_y while K_{26} is symmetric with respect to both, r_x and r_y.

Considering the slow motions on the horizontal plane only, i.e. r_x, r_y and ψ, the methodology herein proposed also allows estimating the corresponding natural periods of oscillations. The natural periods are calculated by solving the corresponding linear eigenvalue problem, by taking the asymptotic limit at zero frequency for the values of the added mass coefficients, also obtained from [26]. Additionally, Table 3 brings the values obtained considering the linearization of the stiffness matrix around the trivial equilibrium position and the comparison with the values presented in the literature. Table 4 brings the structural properties and the

Table 3
Natural periods of oscillation for the trivial position. Unities: s.

	T_1	T_2	T_3
Analytical formulation	76.02	105.48	105.48
Numerical results [26]	76.03	105.53	105.53

Table 4
The OC4-DeepCwind floating platform added masses (at the asymptotic limit at zero frequency).

Mass (m)	1.3473E+7 kg
Platform yaw inertia about CM ($I_{\psi\psi}$)	1.226E+10 kgm^2
Surge-Surge added mass ($M_{a\xi\xi}$)	6.49E+6 kg
Sway-Sway added mass ($M_{a\eta\eta}$)	6.49E+6 kg
Yaw-Yaw added mass ($M_{a\psi\psi}$)	4.87E+9 kgm^2

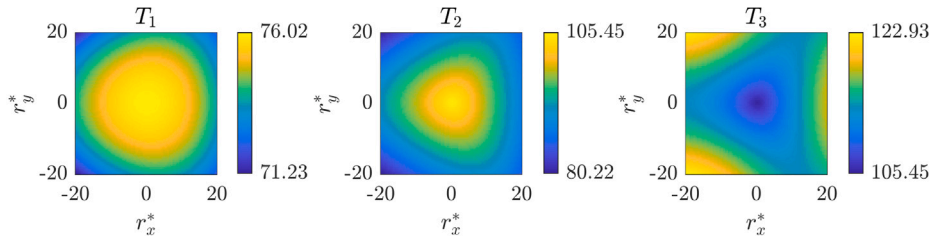

Fig. 7. The OC4-DeepCwind natural periods on the horizontal plane as function of the offset. Unity: s. Offset normalized.

added mass values for the OC4 platform. In this scenario, the corresponding 3×3 stiffness matrix recovers the one obtained by [9]. Notice that in Table 3, the natural periods are enumerated following a crescent order and not that associated with the generalized coordinates. As one could expect, the results show good agreement.

Similarly to the influence on the stiffness coefficients, the mean position may strongly affect natural periods. Such result was already pointed in numerical [14] and physical [15] experiments, taking into account the mean surge position. Fig. 7 brings the colormaps for the natural periods as function of offset position. It is remarkable that the values vary significantly. This demonstrates, once more, the applicability of the present tool, specially in the early stages of design. In fact, the designer usually aims to desynchronize the natural periods of motion from those contained in the excitation. These maps can be used as guiding tools. Again, natural periods maps using OrcaFlex™ can also be assessed. However, as the mass and added mass matrices would not be different, and the differences between analytical and numerical stiffness results are already pointed out as small, the final natural periods map are expected to not differ significantly from the analytically constructed map already presented. For the sake of concision it is not shown in this paper.

Finally, the modes of oscillation for the horizontal plane motions can also be analytically obtained. Fig. 8 brings the natural periods and modes for the trivial equilibrium position ($(r_x^*, r_y^*) = (0, 0)$) and for four shifted positions: $(r_x^*, r_y^*) = (\pm 0.20, \pm 0.20)$. Notice that at the trivial equilibrium position, the modes of oscillation can be seen as "pure", i.e. there is no coupling between the chosen generalized coordinates. This is expected, provided the stiffness matrix considering only these motions is diagonal for that position. In this context, it is possible to recover the ocean engineering classification, from left to right: yaw, sway and surge motions. On the other hand, for the shifted positions, the modes couple those motions. For example, modes 2 and 3 couple surge and sway motions at shifted offset positions. In turn, mode 1, that at the trivial equilibrium position is a pure-yaw mode, becomes a coupled yaw-surge-sway oscillation mode at all shifted positions. Notice also that symmetry patterns of the mooring system arrangement with respect to axis Ox is reproduced on the natural periods, whereas producing an anti-symmetric one for the oscillation modes (e.g., for shifted positions $(r_x^*, r_y^*) = (0.20, 0.20)$ and $(r_x^*, r_y^*) = (0.20, -0.20)$, mode 2 and mode 3 are mirrored with respect to the surge and sway motions, respectively).

The definition of the oscillation modes is useful for the proper understanding of forced responses of the moored vessel. For example, if the oscillations occur around $(r_x^*, r_y^*) = (0.20, -0.20)$ and are resonant with the second mode (i.e, the external force has period T_2), the response has components in surge and yaw, despite being unimodal. The natural modes can also be employed in the Galerkin's method for obtaining reduced-order models (ROMs) that describe the dynamic behavior of the vessel under external static and dynamic loads. Such ROMs exhibit less DOFs than the original equations of motion and, eventually, may have analytical solutions which would be easily programmed in spreadsheets.

4. Conclusions

The present work proposed an analytical and closed-form formulation to obtain the mooring system stiffness. Each mooring line is supposed to be loaded only by conservative forces (gravitational and elastic ones) and linked to holonomous constrains, such

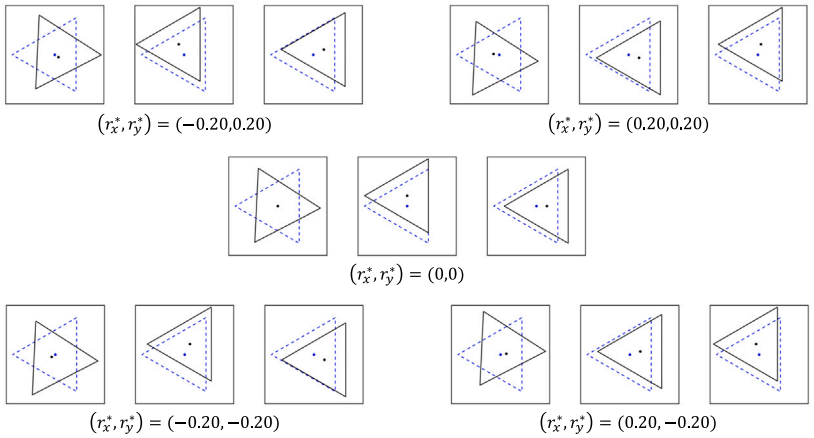

Fig. 8. The OC4-DeepCwind modes of oscillation for the trivial and shifted equilibrium positions, corresponding to natural periods T_j, $j = 1, 2, 3$.

that tension may be written as function of position only. Using classic Analytical Mechanics approaches, the generalized restoring mooring forces are obtained. These forces correspond to the restoring forces acting on the vessel associated to the six generalized coordinates: three translational along x, y and z axes (r_x, r_y and r_z) and three rotational ones (ϕ, θ and ψ). Then, the mooring system stiffness is obtained locally, in a closed analytical form, at any pre-defined position of the vessel. The importance of the present formulation is to provide the designer an analytical tool, easily implementable, able to assess the mooring system stiffness matrix in preliminary design stages. At least to the authors' knowledge, such closed-form, expedite analytical formulation, as well as the developed analysis regarding the effect of the mean position on the stiffness and natural periods are not found in the literature and are novel contributions.

Aiming at illustrating the presented formulation, the OC4-DeepCwind project is taken as a benchmark case study, and an excellent agreement with reported and numerical results has been obtained. For the sake of comparison, maps showing the stiffness coefficients as functions of the pre-defined position are obtained in a few seconds with the analytical formulation. In turn, the same maps are obtained in a few hours if a higher-order hierarchical FEM model is adopted.

Concluding, the methodologies herein proposed may be of great value for the design and further operation of mooring system projects. The analytic and expedite formulations allow the designer to easily vary parameters in order to evaluate their impact on the response of the whole system, allowing for comprehensive sensitivity studies regarding the mooring system stiffness. This can help more advanced and sophisticated numerical analyses, contributing for the viability of the project. Considering operations, active winch performances can be planned to desynchronize the natural periods from excitation, for instance. Further work may include: (i) nonlinear dynamic analysis, bifurcation and equilibrium stability studies; (ii) VIM studies, based on reduced order models and respective susceptibility maps; (iii) parametric optimization of mooring systems, based on the non linear behavior of the system; (iv) digital twins of mooring systems, including health monitoring based on predicted and actual behavior; (v) an expansion of the analytical model to take into account possible shared lines between two adjacent moored units.

Declaration of competing interest

The authors declare that they have no known competing financial interests or personal relationships that could have appeared to influence the work reported in this paper.

Acknowledgments

The first author acknowledges ONRG for MSc scholarship in the context of ONRG project nr. N62909-16-1-2066. The second and the third authors refer to the Brazilian Research Council (CNPq), research grants 308230/2018-3 and 305945/2020-3. This paper is part of the activities developed in a bilateral research project sponsored by CAPES, Brazil and JSPS, grant 88881.191007/2018-01. Petrobras is also acknowledged.

Appendix. Mooring system stiffness coefficients

Coefficients at the grounded reference frame O_{xyz} are:

• First line coefficients — coefficients associated with a displacement in r_x:

$$K_{11}^{(i)} = k_{HH}^{(i)} \cos^2 \alpha^{(i)} + \bar{k}_{HH}^{(i)} \sin^2 \alpha^{(i)} \tag{44}$$

$$K_{12}^{(i)} = \left(k_{HH}^{(i)} - \bar{k}_{HH}^{(i)} \right) \cos \alpha^{(i)} \sin \alpha^{(i)} \tag{45}$$

$$K_{13}^{(i)} = -k_{HV}^{(i)} \cos\alpha^{(i)} \tag{46}$$

$$K_{14}^{(i)} = \frac{\partial p_x^{(i)}}{\partial \phi} K_{11}^{(i)} + \frac{\partial p_y^{(i)}}{\partial \phi} K_{12}^{(i)} + \frac{\partial p_z^{(i)}}{\partial \phi} K_{13}^{(i)} \tag{47}$$

$$K_{15}^{(i)} = \frac{\partial p_x^{(i)}}{\partial \theta} K_{11}^{(i)} + \frac{\partial p_y^{(i)}}{\partial \theta} K_{12}^{(i)} + \frac{\partial p_z^{(i)}}{\partial \theta} K_{13}^{(i)} \tag{48}$$

$$K_{16}^{(i)} = \frac{\partial p_x^{(i)}}{\partial \psi} K_{11}^{(i)} + \frac{\partial p_y^{(i)}}{\partial \psi} K_{12}^{(i)} \tag{49}$$

- Second line coefficients — coefficients associated with a displacement in r_y:

$$K_{21}^{(i)} = \sum_{i=1}^{N} \left(k_{HH}^{(i)} - \bar{k}_{HH}^{(i)} \right) \sin\alpha^{(i)} \cos\alpha^{(i)} \tag{50}$$

$$K_{22}^{(i)} = k_{HH}^{(i)} \sin^2\alpha^{(i)} + \bar{k}_{HH}^{(i)} \cos^2\alpha^{(i)} \tag{51}$$

$$K_{23}^{(i)} = -k_{HV}^{(i)} \sin\alpha^{(i)} \tag{52}$$

$$K_{24}^{(i)} = \frac{\partial p_x^{(i)}}{\partial \phi} K_{21}^{(i)} + \frac{\partial p_y^{(i)}}{\partial \phi} K_{22}^{(i)} + \frac{\partial p_z^{(i)}}{\partial \phi} K_{23}^{(i)} \tag{53}$$

$$K_{25}^{(i)} = \frac{\partial p_x^{(i)}}{\partial \theta} K_{21}^{(i)} + \frac{\partial p_y^{(i)}}{\partial \theta} K_{22}^{(i)} + \frac{\partial p_z^{(i)}}{\partial \theta} K_{23}^{(i)} \tag{54}$$

$$K_{26}^{(i)} = \frac{\partial p_x^{(i)}}{\partial \psi} K_{21}^{(i)} + \frac{\partial p_y^{(i)}}{\partial \psi} K_{22}^{(i)} \tag{55}$$

- Third line coefficients — coefficients associated with a displacement in r_z:

$$K_{31}^{(i)} = -k_{VH}^{(i)} \cos\alpha^{(i)} \tag{56}$$

$$K_{32}^{(i)} = -k_{VH}^{(i)} \sin\alpha^{(i)} \tag{57}$$

$$K_{33}^{(i)} = k_{VV}^{(i)} \tag{58}$$

$$K_{34}^{(i)} = \frac{\partial p_x^{(i)}}{\partial \phi} K_{31}^{(i)} + \frac{\partial p_y^{(i)}}{\partial \phi} K_{32}^{(i)} + \frac{\partial p_z^{(i)}}{\partial \phi} K_{33}^{(i)} \tag{59}$$

$$K_{35}^{(i)} = \frac{\partial p_x^{(i)}}{\partial \theta} K_{31}^{(i)} + \frac{\partial p_y^{(i)}}{\partial \theta} K_{32}^{(i)} + \frac{\partial p_z^{(i)}}{\partial \theta} K_{33}^{(i)} \tag{60}$$

$$K_{36}^{(i)} = \frac{\partial p_x^{(i)}}{\partial \psi} K_{31}^{(i)} + \frac{\partial p_y^{(i)}}{\partial \psi} K_{32}^{(i)} \tag{61}$$

- Fourth line coefficients — coefficients associated with a displacement in ϕ:

$$K_{41}^{(i)} = \frac{\partial p_x^{(i)}}{\partial \phi} K_{11}^{(i)} + \frac{\partial p_y^{(i)}}{\partial \phi} K_{12}^{(i)} + \frac{\partial p_z^{(i)}}{\partial \phi} K_{13}^{(i)} \tag{62}$$

$$K_{42}^{(i)} = \frac{\partial p_x^{(i)}}{\partial \phi} K_{21}^{(i)} + \frac{\partial p_y^{(i)}}{\partial \phi} K_{22}^{(i)} + \frac{\partial p_z^{(i)}}{\partial \phi} K_{23}^{(i)} \tag{63}$$

$$K_{43}^{(i)} = \frac{\partial p_x^{(i)}}{\partial \phi} K_{31}^{(i)} + \frac{\partial p_y^{(i)}}{\partial \phi} K_{32}^{(i)} + \frac{\partial p_z^{(i)}}{\partial \phi} K_{33}^{(i)} \tag{64}$$

$$K_{44}^{(i)} = \frac{\partial p_x^{(i)}}{\partial \phi} K_{14}^{(i)} + \frac{\partial p_y^{(i)}}{\partial \phi} K_{24}^{(i)} + \frac{\partial p_z^{(i)}}{\partial \phi} K_{34}^{(i)} - \frac{\partial^2 p_x^{(i)}}{\partial \phi^2} F_H^{(i)} \cos\alpha^{(i)} - \frac{\partial^2 p_y^{(i)}}{\partial \phi^2} F_H^{(i)} \sin\alpha^{(i)} + \frac{\partial^2 p_z^{(i)}}{\partial \phi^2} F_V^{(i)} \tag{65}$$

$$K_{45}^{(i)} = \frac{\partial p_x^{(i)}}{\partial \phi} K_{15}^{(i)} + \frac{\partial p_y^{(i)}}{\partial \phi} K_{25}^{(i)} + \frac{\partial p_z^{(i)}}{\partial \phi} K_{35}^{(i)} - \frac{\partial^2 p_x^{(i)}}{\partial \phi \partial \theta} F_H^{(i)} \cos\alpha^{(i)} - \frac{\partial^2 p_y^{(i)}}{\partial \phi \partial \theta} F_H^{(i)} \sin\alpha^{(i)} + \frac{\partial^2 p_z^{(i)}}{\partial \phi \partial \theta} F_V^{(i)} \tag{66}$$

$$K_{46}^{(i)} = \frac{\partial p_x^{(i)}}{\partial \phi} K_{16}^{(i)} + \frac{\partial p_y^{(i)}}{\partial \phi} K_{26}^{(i)} + \frac{\partial p_z^{(i)}}{\partial \phi} K_{36}^{(i)} - \frac{\partial^2 p_x^{(i)}}{\partial \phi \partial \psi} F_H^{(i)} \cos\alpha^{(i)} - \frac{\partial^2 p_y^{(i)}}{\partial \phi \partial \psi} F_H^{(i)} \sin\alpha^{(i)} + \frac{\partial^2 p_z^{(i)}}{\partial \phi \partial \psi} F_V^{(i)} \tag{67}$$

- Fifth line coefficients — coefficients associated with a displacement in θ:

$$K_{51}^{(i)} = \frac{\partial p_x^{(i)}}{\partial \theta} K_{11}^{(i)} + \frac{\partial p_y^{(i)}}{\partial \theta} K_{12}^{(i)} + \frac{\partial p_z^{(i)}}{\partial \theta} K_{13}^{(i)} \tag{68}$$

$$K_{52}^{(i)} = \frac{\partial p_x^{(i)}}{\partial \theta} K_{21}^{(i)} + \frac{\partial p_y^{(i)}}{\partial \theta} K_{22}^{(i)} + \frac{\partial p_z^{(i)}}{\partial \theta} K_{23}^{(i)} \tag{69}$$

$$K_{53}^{(i)} = \frac{\partial p_x^{(i)}}{\partial \theta} K_{31}^{(i)} + \frac{\partial p_y^{(i)}}{\partial \theta} K_{32}^{(i)} + \frac{\partial p_z^{(i)}}{\partial \theta} K_{33}^{(i)} \tag{70}$$

$$K_{54}^{(i)} = \frac{\partial p_x^{(i)}}{\partial \theta} K_{14}^{(i)} + \frac{\partial p_y^{(i)}}{\partial \theta} K_{24}^{(i)} + \frac{\partial p_z^{(i)}}{\partial \theta} K_{34}^{(i)} - \frac{\partial^2 p_x^{(i)}}{\partial \theta \partial \phi} F_H^{(i)} \cos\alpha^{(i)} - \frac{\partial^2 p_y^{(i)}}{\partial \theta \partial \phi} F_H^{(i)} \sin\alpha^{(i)} + \frac{\partial^2 p_z^{(i)}}{\partial \theta \partial \phi} F_V^{(i)} \tag{71}$$

$$K_{55}^{(i)} = \frac{\partial p_x^{(i)}}{\partial \theta} K_{15}^{(i)} + \frac{\partial p_y^{(i)}}{\partial \theta} K_{25}^{(i)} + \frac{\partial p_z^{(i)}}{\partial \theta} K_{35}^{(i)} - \frac{\partial^2 p_x^{(i)}}{\partial \theta^2} F_H^{(i)} \cos\alpha^{(i)} - \frac{\partial^2 p_y^{(i)}}{\partial \theta^2} F_H^{(i)} \sin\alpha^{(i)} + \frac{\partial^2 p_z^{(i)}}{\partial \theta^2} F_V^{(i)} \tag{72}$$

$$K_{56}^{(i)} = \frac{\partial p_x^{(i)}}{\partial \theta} K_{16}^{(i)} + \frac{\partial p_y^{(i)}}{\partial \theta} K_{26}^{(i)} + \frac{\partial p_z^{(i)}}{\partial \theta} K_{36}^{(i)} - \frac{\partial^2 p_x^{(i)}}{\partial \theta \partial \psi} F_H^{(i)} \cos\alpha^{(i)} - \frac{\partial^2 p_y^{(i)}}{\partial \theta \partial \psi} F_H^{(i)} \sin\alpha^{(i)} + \frac{\partial^2 p_z^{(i)}}{\partial \theta \partial \psi} F_V^{(i)} \tag{73}$$

- Sixth line coefficients — coefficients associated with a displacement in ψ:

$$K_{61}^{(i)} = \frac{\partial p_x^{(i)}}{\partial \psi} K_{11^{(i)}} + \frac{\partial p_y^{(i)}}{\partial \psi} K_{12}^{(i)} \tag{74}$$

$$K_{62}^{(i)} = \frac{\partial p_x^{(i)}}{\partial \psi} K_{21}^{(i)} + \frac{\partial p_y^{(i)}}{\partial \psi} K_{22}^{(i)} \tag{75}$$

$$K_{63}^{(i)} = \frac{\partial p_x^{(i)}}{\partial \psi} K_{31}^{(i)} + \frac{\partial p_y^{(i)}}{\partial \psi} K_{32}^{(i)} \tag{76}$$

$$K_{64}^{(i)} = \frac{\partial p_x^{(i)}}{\partial \psi} K_{14}^{(i)} + \frac{\partial p_y^{(i)}}{\partial \psi} K_{24}^{(i)} - \frac{\partial^2 p_x^{(i)}}{\partial \psi \partial \phi} F_H^{(i)} \cos\alpha^{(i)} - \frac{\partial^2 p_y^{(i)}}{\partial \psi \partial \phi} F_H^{(i)} \sin\alpha^{(i)} \tag{77}$$

$$K_{65}^{(i)} = \frac{\partial p_x^{(i)}}{\partial \psi} K_{15}^{(i)} + \frac{\partial p_y^{(i)}}{\partial \psi} K_{25}^{(i)} - \frac{\partial^2 p_x^{(i)}}{\partial \psi \partial \theta} F_H^{(i)} \cos\alpha^{(i)} - \frac{\partial^2 p_y^{(i)}}{\partial \psi \partial \theta} F_H^{(i)} \sin\alpha^{(i)} \tag{78}$$

$$K_{66}^{(i)} = \frac{\partial p_x^{(i)}}{\partial \psi} K_{14}^{(i)} + \frac{\partial p_y^{(i)}}{\partial \psi} K_{24}^{(i)} - \frac{\partial^2 p_x^{(i)}}{\partial \psi^2} F_H^{(i)} \cos\alpha^{(i)} - \frac{\partial^2 p_y^{(i)}}{\partial \psi^2} F_H^{(i)} \sin\alpha^{(i)} \tag{79}$$

For stiffness coefficients at the moving reference frame $G_{\xi\eta\zeta}$, it is necessary to rotate the matrix as follows:

$$[\mathbb{K}]_{E_\xi} = [\mathbb{R}^*]^t [\mathbb{K}]_{E_x} [\mathbb{R}^*] \tag{80}$$

where:

$$[\mathbb{R}^*] = \left(\begin{array}{c|c} [\mathbb{R}]_{E_x|E_\xi} & 0 \\ \hline 0 & [\mathbb{I}] \end{array} \right) \tag{81}$$

with $[\mathbb{I}]$ being the 3×3 identity matrix (Eq. (82)).

$$[\mathbb{R}]_{E_x|E_\xi} = \begin{pmatrix} \cos\theta\cos\psi & \sin\phi\sin\theta\cos\psi - \cos\phi\sin\psi & \cos\phi\sin\theta\cos\psi + \sin\phi\sin\psi \\ \cos\theta\sin\psi & \sin\phi\sin\theta\sin\psi + \cos\phi\cos\psi & \cos\phi\sin\theta\sin\psi - \sin\phi\cos\psi \\ -\sin\theta & \sin\phi\cos\theta & \cos\phi\cos\theta \end{pmatrix} \tag{82}$$

References

[1] Xu Kun, Larsen Kjell, Shao Yanlin, Zhang Min, Gao Zhen, Moan Torgeir. Design and comparative analysis of alternative mooring systems for floating wind turbines in shallow water with emphasis on ultimate limit state design. Ocean Eng 2021;129:108377. http://dx.doi.org/10.1016/j.oceaneng.2020.108377.

[2] Bureau Veritas. BV NR493 classification of mooring systems for permanet and mobile offshore units, DT R03 E, december 2015. 2015.

[3] Yamamoto Tokuo, Yoshida Akinori, Ijima Takeshi. Dynamics of elastically moored floating objects. Appl Ocean Res 1980;2(2):85–92. http://dx.doi.org/10.1016/0141-1187(80)90034-6.

[4] Pesce Celso P. Preliminary analysis of moored system dynamics (in portuguese). Techreport n. 77, IPT – Technological Research Institute of the State of São Paulo; 1986.

[5] Faltinsen O. Sea loads on ships and offshore structures. In: Cambridge ocean technology series, Cambridge University Press; 1993, URL https://books.google.com.br/books?id=qZq4Rs2DZXoC.

[6] Sannasiraj SA, Sundar V, Sundaravadivelu R. Mooring forces and motion responses of pontoon-type floating breakwaters. Ocean Eng 1998;25(1):27–48. http://dx.doi.org/10.1016/s0029-8018(96)00044-3.

[7] Montasir OA, Yenduri A, Kurian VJ. Effect of mooring line configurations on the dynamic responses of truss spar platforms. Ocean Eng 2015;96:161–72. http://dx.doi.org/10.1016/j.oceaneng.2014.11.027.

[8] Gutiérrez-Romero José E, García-Espinosa Julio, Serván-Camas Borja, Zamora-Parra Blas. Non-linear dynamic analysis of the response of moored floating structures. Mar Struct 2016;49:116–37. http://dx.doi.org/10.1016/j.marstruc.2016.05.002.

[9] Pesce Celso P, Amaral Giovanni A, Franzini Guilherme R. Mooring system stiffness: A general analytical formulation with an application to floating offshore wind turbines. In: ASME 2018 1st international offshore wind technical conference. ASME; 2018, http://dx.doi.org/10.1115/iowtc2018-1040.

[10] Loukogeorgaki Eva, Angelides Demos C. Stiffness of mooring lines and performance of floating breakwater in three dimensions. Appl Ocean Res 2005;27(4–5):187–208. http://dx.doi.org/10.1016/j.apor.2005.12.002.

[11] Kim Byoung Wan, Sung Hong Gun, Kim Jin Ha, Hong Sa Young. Comparison of linear spring and nonlinear FEM methods in dynamic coupled analysis of floating structure and mooring system. J Fluids Struct 2013;42:205–27. http://dx.doi.org/10.1016/j.jfluidstructs.2013.07.002.

[12] Robertson A, Jonkman J, Masciola M, Song H, Goupee A, Coulling A, et al. Definition of the semisubmersible floating system for phase II of OC4. Technical report, Office of Scientific and Technical Information (OSTI); 2014, http://dx.doi.org/10.2172/1155123.

[13] Al-Solihat Mohammed Khair, Nahon Meyer. Stiffness of slack and taut moorings. Ships Offshore Struct 2015;11(8):890–904. http://dx.doi.org/10.1080/17445302.2015.1089052.

[14] Souza CE, Bachynski EE. Changes in surge and pitch decay periods of floating wind turbines for varying wind speed. Ocean Eng 2019;180:223–37. http://dx.doi.org/10.1016/j.oceaneng.2019.02.075.

[15] Amaral Giovanni A, Mello Pedro C, do Carmo Lucas HS, Alberto Izabela F, Malta Edgard B, Simos Alexandre N, et al. Seakeeping tests of a FOWT in wind and waves: An analysis of dynamic coupling effects and their impact on the predictions of pitch motion response. J Mar Sci Eng 2021;9:197. http://dx.doi.org/10.3390/jmse9020179.

[16] Pesce Celso P, Amaral Giovanni A, Mendes Bruno, Oliveira Everton L, Franzini Guilherme R. A model to assess the susceptibility of a multicolumn FOWT platform to vortex-induced motions in early design stages. In: ASME 2021 40th international conference on ocean, offshore and arctic engineering. ASME; 2021.

[17] Bach-Gansmo Magnus Thorsen, Garvik Stian Kielland, Thomsen Jonas Bjerg, Andersen Morten Thøtt. Parametric study of a taut compliant mooring system for a FOWT compared to a catenary mooring. J Mar Sci Eng 2020;8(6). http://dx.doi.org/10.3390/jmse8060431, URL https://www.mdpi.com/2077-1312/8/6/431.

[18] Suzuki Hideyuki, Shiohara Hiroki, Schnepf Anja, Houtani Hidetaka, Carmo Lucas HS, Hirabayashi Shinichiro, et al. Wave and wind responses of a very-light FOWT with guy-wired-supported tower: Numerical and experimental studies. J Mar Sci Eng 2020;8(11). http://dx.doi.org/10.3390/jmse8110841, URL https://www.mdpi.com/2077-1312/8/11/841.

[19] Takata Taisuke, Takaoka Mayuko, Gonçalves Rodolfo T, Houtani Hidetaka, Yoshimura Yasuo, Hara Kentaro, et al. Dynamic behavior of a flexible multi-column FOWT in regular waves. J Mar Sci Eng 2021;9(2). http://dx.doi.org/10.3390/jmse9020124, URL https://www.mdpi.com/2077-1312/9/2/124.

[20] Gonçalves Rodolfo T, Chame Maria EF, Silva Leandro SP, Koop Arjen, Hirabayashi Shinichiro, Suzuki Hideyuki. Experimental flow-induced motions of a FOWT semi-submersible type (OC4 phase II floater). J Offshore Mech Arct Eng 2020;143(1). http://dx.doi.org/10.1115/1.4048149, arXiv:https://asmedigitalcollection.asme.org/offshoremechanics/article-pdf/143/1/012004/6562494/omae_143_1_012004.pdf.

[21] Lanczos Cornelius. The variational principles of mechanics. Dover Publications Inc. 1986, URL https://www.ebook.de/de/product/1925571/cornelius_lanczos_the_variational_principles_of_mechanics.html.

[22] Amaral Giovanni Aiosa. Analytical assessment of the mooring system stiffness. Master's thesis. Escola Politécnica da Universidade de São Paulo; 2020, http://dx.doi.org/10.11606/D.3.2020.tde-05112020-114447.

[23] Orcina. OrcaFlex web help. 2011, URL https://www.orcina.com/webhelp/OrcaFlex/.

[24] Bernitsas MM, Garza-Rios LO. Effect of mooring line arrangement on the dynamics of spread mooring systems. J Offshore Mech Arct Eng 1996;118(1):7. http://dx.doi.org/10.1115/1.2828806.

[25] Bernitsas MM, Kim B-K. Effect of slow-drift loads on nonlinear dynamics of spread mooring systems. J Offshore Mech Arct Eng 1998;120(4):201. http://dx.doi.org/10.1115/1.2829541.

[26] Robertson Amy, Jonkman Jason, Vorpahl Fabian, Popko Wojciech, Qvist Jacob, Frøyd Lars, et al. Offshore code comparison collaboration continuation within IEA wind task 30: Phase II results regarding a floating semisubmersible wind system. In: Volume 9B: ocean renewable energy. ASME; 2014, http://dx.doi.org/10.1115/omae2014-24040.